Flutter and Buffeting Analysis of Bridges Subjected to Skew Wind

Ming-Hui Huang*, Yuh-Yi Lin and Ming-Xi Weng

Department of Civil Engineering, Tamkang University,
Tamsui, Taiwan 251, R.O.C.

Abstract

This paper aims to study the aerodynamic behavior of bridges under skew wind by performing a series of section model tests and a numerical analysis. Two types of deck cross sections, with the width-to-depth (B/H) ratios of 5 and 10, were used in the test and the numerical analysis. The section model tests included measurements of the aerodynamic coefficients and flutter derivatives, the flutter critical wind speeds, and the buffeting responses. The effects of yaw angles were investigated both in the tests and the numerical analysis. The experimental results show that for the section model with B/H ratio of 5, the lowest flutter wind speed occurs at a negative angle of wind attack and a zero yaw angle. For the section model with B/H ratio of 10, the lowest flutter wind speed occurs at a negative angle of wind attack and a yaw angle of 20 degrees. These results also indicate that in the case of zero angle of wind attack, the flutter critical wind speeds increase with the yaw angles and the buffeting responses decrease as the yaw angles increase. To verify the applicability and validity of this analytical approach, an example is provided. Comparisons show that the calculated results obtained from this approach follow the same trend with the experimental results. The results obtained from the conventional method (mean wind decomposition) may not be applicable for large yaw angles.

Key Words: Flutter, Buffeting, Bridge, Wind Tunnel Test, Skew Wind

1. Introduction

The developments of construction techniques and high strength materials have made the type of cable-supported bridges to become a favorable choice for bridge design. The considerations of design of this type of bridges are not only basic functions but also aesthetics. Therefore, some curved bridges emphasizing attractive appearances were built. For these curved bridges subjected to wind excitations, the effects of yaw angles on the aerodynamic behavior become important. Thus, an analytical approach based on flutter and buffeting theory of bridges under skew wind is needed, and it should be examined before applied to the curved bridges. Although many studies [1−9] have focused on the aerodynamic behavior of bridges under skew wind, the observations and findings from their studies were not consistent because of different cross sections of bridge deck. For practical use, an analytical approach based on the measured coefficients from section model tests is a relatively easy method and costs less. Therefore, this paper aims to study the aerodynamic behavior of bridges under skew wind by performing a series of section model tests and a numerical analysis. Using the results in this paper, an approach to analyze the aerodynamic behavior of curved bridges will be possible and will be investigated in the near future.

The conventional theories and wind tunnel tests for investigating flutter critical wind speeds and buffeting responses of bridges were established based on the assumption that the mean wind direction was normal to the longitudinal axis of the bridge deck. The assumption has

*Corresponding author. E-mail: fansu0609@gmail.com

been well accepted because it is considered as the worst case. However, Tanaka and Davenport [1] performed a taut strip model test and found that the buffeting responses of the bridge under yaw angles were larger than those under normal condition. Zhu et al. [2] performed a full bridge model test and indicated that the unfavorable buffeting responses of the bridge may occur in the cases of the bridge subjected to skew wind. Zhu and Chang [3] pointed out that the lowest flutter wind speeds of the bridges may occur in the cases of the bridges under yaw winds at non-zero angles of wind attack. Traditionally, mean wind decomposition is often adopted to study the aerodynamic behavior of bridges under skew wind [4,5]. However, Zhu et al. [6,7] pointed out that this conventional method can be only applied to the cases with small yaw angles. They found that the decomposition method underestimated the aerodynamic coefficients and the errors increased with yaw angles. In their papers, a testing frame was set up to measure aerodynamic coefficients and flutter derivatives. A comparison was made between their results and those obtained from the conventional methods. Xu etc. [8] used this approach to analyze the Ting-Ma Bridge under skew wind and compared the results with those obtained from field measurements. Scanlan [10] proposed a simplified approach for determining the flutter critical wind speeds of bridges to skew wind. However, the method is only valid in the case of bridges to small yaw angles [7].

In this paper, the analytical model based on the aerodynamic coefficients and the flutter derivatives, measured from section model tests with different yaw angles, is used to predict the flutter critical wind speed and buffeting responses of the bridge under skew wind. Two types of bridge deck cross sections respectively with the width-to-depth (B/H) ratios of 5 and 10 were used both in the section model tests and in the numerical analysis. A bridge example, representing a straight bridge under skew wind, is provided to verify the applicability and validity of this approach. Analytical results are compared with those obtained from the wind tunnel test and the decomposition method.

2. Formulations of Flutter and Buffeting

In the formulations, there are two coordinate systems introduced. One is the global coordinate system XYZ, the other is the mean wind coordinate system $X_W Y_W Z_W$ (shown in Figure 1). The forces expressed in the mean wind coordinate system can be transformed into those in the global coordinate system by using the transformation matrix T. The relationship between these forces can be stated as follows:

$$\begin{bmatrix} A & L & D & M_X & M_Y & M_Z \end{bmatrix}^T = \begin{bmatrix} \mathbf{T} & \mathbf{0} \\ \mathbf{0} & \mathbf{T} \end{bmatrix} \begin{bmatrix} A_W & L_W & D_W & M_{XW} & M_{YW} & M_{WZ} \end{bmatrix}^T \tag{1}$$

where A, L, D, and M_k are the axial force, the vertical force, the drag force, and the moment about k (k = x or y or z) axis in the global coordinate system, respectively; the subscript w designates the force in the mean wind coordinate system; the transformation matrix T is stated as:

$$\mathbf{T} = \begin{bmatrix} \cos\beta & -\sin\alpha\sin\beta & \cos\alpha\sin\beta \\ 0 & \cos\alpha & \sin\alpha \\ -\sin\beta & -\sin\alpha\cos\beta & \cos\alpha\cos\beta \end{bmatrix} \tag{2}$$

in which α is the angle of wind attack, β is the yaw angle.

The equation of motion of a bridge subjected to wind excitations, referred to the global coordinate system, can be stated in a matrix form as follows:

$$\mathbf{M}\ddot{\mathbf{D}}(t) + \mathbf{C}\dot{\mathbf{D}}(t) + \mathbf{K}\mathbf{D}(t) = \mathbf{F}^s(t) + \mathbf{F}^b(t) \tag{3}$$

where $\mathbf{D}(t)$ is the nodal displacement vector, $\dot{\mathbf{D}}(t)$ and $\ddot{\mathbf{D}}(t)$ are the vectors of the nodal velocity and acceleration, respectively, **M**, **C**, and **K** are the matrices of mass, damping, and stiffness, respectively, $\mathbf{F}^s$ is the self-ex-

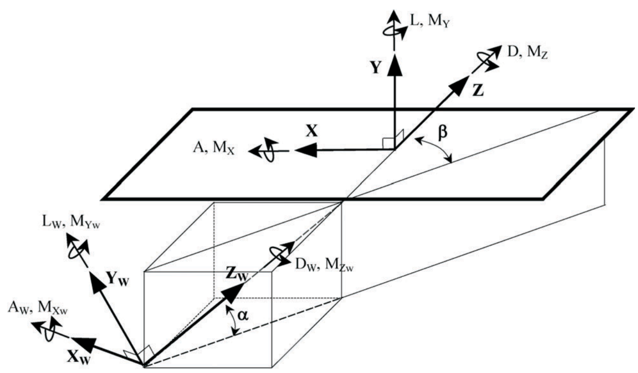

Figure 1. Coordinate systems.

cited force vector, $\mathbf{F}^b$ is the buffeting force vector.

In the flutter analysis, the buffeting force is not included in Eq. (3) because flutter is related to the aerodynamic damping and stiffness that are induced by the self-excited force only. In the conventional expressions [11], the self-excited moments about axes Y and Z, and the axial force are always neglected. It is because these forces are relatively small compared to the other terms. Therefore, the major self-excited forces in the vertical, drag, and torsional directions are only taken into account in this study. These self-excited forces acting on the bridge per unit deck length are expressed in the global coordinate system as follows:

$$L^{se} = \rho U^2 BK\left[H_1^*(\alpha,\beta,K)\frac{\dot{y}}{U} + H_2^*(\alpha,\beta,K)\frac{\dot{\theta}_x}{U} + KH_3^*(\alpha,\beta,K)\theta_x + KH_4^*(\alpha,\beta,K)\frac{y}{B}\right] \tag{4}$$

$$D^{se} = \rho U^2 BK\left[P_1^*(\alpha,\beta,K)\frac{\dot{z}}{U} + P_2^*(\alpha,\beta,K)\frac{\dot{\theta}_x}{U} + KP_3^*(\alpha,\beta,K)\theta_x + P_4^*(\alpha,\beta,K)\frac{z}{B}\right] \tag{5}$$

$$M_x^{se} = \rho U^2 B^2 K\left[A_1^*(\alpha,\beta,K)\frac{\dot{y}}{U} + A_2^*(\alpha,\beta,K)\frac{\dot{\theta}_x}{U} + KA_3^*(\alpha,\beta,K)\theta_x + KA_4^*(\alpha,\beta,K)\frac{y}{B}\right] \tag{6}$$

where the superscript se represents the self-excited force; $K = \omega B/U$ is the reduced frequency; ω, ρ, B, and U are circular frequency, air density, width of bridge deck, and mean wind velocity, respectively; y, z, and θ_x are the displacements of Y, Z, and the rotation of X axes, respective; $H_i^*(\alpha,\beta,K)$, $P_i^*(\alpha,\beta,K)$ and $A_i^*(\alpha,\beta,K)$ (i = 1~4) are the flutter derivatives defined in the global coordinate system with combinations of α and β. The measurements of flutter derivatives in the tests were performed in the way conforming to Eq. (4)–(6). Then, substituting the self-excited forces into the equation of motion, Eq. (3), the aerodynamic stiffness and aerodynamic damping effects are incorporated with the structural system. The system natural frequency and critical velocity for onset of flutter critical wind speed can be found by using the complex eigen-value analysis.

In the buffeting analysis, both self-excited force and buffeting force are taken into considerations. The buffeting moments about axes Y and Z, and the axial force are also neglected because of the same reasons mentioned above in the flutter analysis. According to the assumption of quasi-steady theory, the major fluctuating forces acting on the bridge per unit deck length can be derived in the mean wind coordinate system as follows:

$$D_W^b = \frac{1}{2}\rho U^2 B\left[C_{Dw}(\alpha,\beta)\frac{2u}{U} + \left(\left.\frac{\partial C_{Dw}}{\partial\beta}\right|_{\alpha,\beta} - C_{Aw}(\alpha,\beta)\right)\frac{v}{U} + \left(\left.\frac{\partial C_{Dw}}{\partial\alpha}\right|_{\alpha,\beta} - C_{Lw}(\alpha,\beta)\right)\frac{w}{U}\right] \tag{7}$$

$$L_W^b = \frac{1}{2}\rho U^2 B\left[C_{Lw}(\alpha,\beta)\frac{2u}{U} + \left.\frac{\partial C_{Lw}}{\partial\beta}\right|_{\alpha,\beta}\frac{v}{U} + \left(\left.\frac{\partial C_{Lw}}{\partial\alpha}\right|_{\alpha,\beta} + C_{Dw}(\alpha,\beta)\right)\frac{w}{U}\right] \tag{8}$$

$$M_W^b = \frac{1}{2}\rho U^2 B^2\left[C_{Mxw}(\alpha,\beta)\frac{2u}{U} + \left(\left.\frac{\partial C_{Mxw}}{\partial\beta}\right|_{\alpha,\beta} + C_{Mzw}(\alpha,\beta)\right)\frac{v}{U} + \left.\frac{\partial C_{Mxw}}{\partial\alpha}\right|_{\alpha,\beta}\frac{w}{U}\right] \tag{9}$$

where u, v, and w are the wind velocity fluctuations in the drag, lateral, and vertical directions, respectively; C_{Aw}, C_{Lw}, and C_{Dw} are the force coefficients with respect to axes X_W, Y_W, and Z_W, respectively. C_{Mxw}, C_{Myw} are the moment coefficients with respect to axes X_W and Y_W, respectively. The aerodynamic coefficients are defined as:

$$C_{Aw} = A_W \Big/ \frac{1}{2}\rho U^2 BL,\quad C_{Lw} = L_W \Big/ \frac{1}{2}\rho U^2 BL,\quad C_{Dw} = D_W \Big/ \frac{1}{2}\rho U^2 BL \tag{10}$$

$$C_{Mxw} = M_{XW} \Big/ \frac{1}{2}\rho U^2 B^2 L,\quad C_{Myw} = M_{YW} \Big/ \frac{1}{2}\rho U^2 B^2 L,\quad C_{Mzw} = M_{ZW} \Big/ \frac{1}{2}\rho U^2 B^2 L \tag{11}$$

where L is the length of section model. It should be noted that all the buffeting forces, expressed in Eq. (7)–(9), are formed in the mean wind coordinate system and should be converted into the forces in the global coordinate system for the buffeting analysis. The transformation of the forces can be done by using Eq. (1). After the force spectrum is formed, then the dynamic responses can be obtained through a simple spectral analysis [11].

3. Section Model Tests

The section model tests were conducted in the First Wind Tunnel in Tamkang University. The wind tunnel has a working section of 1.5 m(W) × 1.8 m(H) × 7.4 m(L). Two rectangular cross sections of bridge deck, respectively with the B/H ratios of 5 and 10, were tested. The aerodynamic coefficients and flutter derivatives of these models were measured under smooth flow. The yaw angles, ranged from 0 to 30 degrees at an interval of 7.5 degrees, and the angles of wind attack, ranged from -9 degrees to 9 degrees at an interval of 1 or 2 degrees, were considered in the testing of aerodynamic coefficients. Only yaw angles, ranged from 0 to 30 degrees at an interval of 10 degrees, were considered in the testing of flutter derivatives where the angle of wind attack was zero.

The configuration for measuring the aerodynamic coefficients is shown in Figure 2. This testing frame is similar to that described in the literature [6] with some modifications. The section model was vertically installed in the wind tunnel. To facilitate the test for different yaw angles, the rectangular segment of the section model was made. For the cases with yaw angles, two wedge segments were respectively attached to the section model at the top and bottom of the section model to make the tested model as a parallelogram. The bottom of the section model was connected with a force balance. A steel plate, used for adjusting yaw angles, was placed between the force balance and the tuning table. To reduce 3D flow effects, an end plate was placed on the top of the section model and the floor of the wind tunnel around the bottom of the section model was elevated. Changes of angles of wind attack can be achieved by rotating the tuning table. In this configuration, the forces of six components were measured with respect to the local coordinate system of the bridge deck. Since the force balance was installed at the bottom of the section model, the measured forces were transformed to those with respect to the mean wind coordinate system with the origin at the gravity center. Then, these forces were used for the calculation of the aerodynamic coefficients C_{Dw}, C_{Lw}, and C_{Mxw}.

The configuration for measuring flutter derivatives is shown in Figure 3. This testing frame is similar to that described in the literature [7]. The spring-supported section model was suspended in the wind tunnel. For the tests with different yaw angles, the fixed positions of the springs on the ceiling were adjusted by using the curved rails which were attached with the ceiling. To assure the edges of the test models being parallel to wind, two segments were connected with the section model on both sides. The displacements of the section model were measured by the displacement sensors installed on the top of the section model. Using MITD [12,13], the flutter derivatives were then identified from the free vibrations. The measured aerodynamic coefficients and flutter derivatives were then substituted into the analytical model

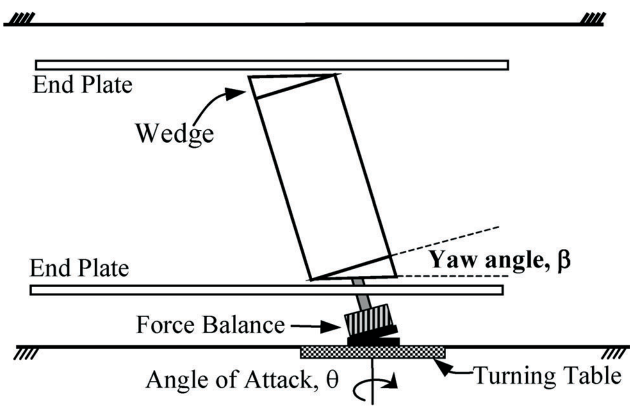

Figure 2. Configuration for measuring aerodynamic coefficients.

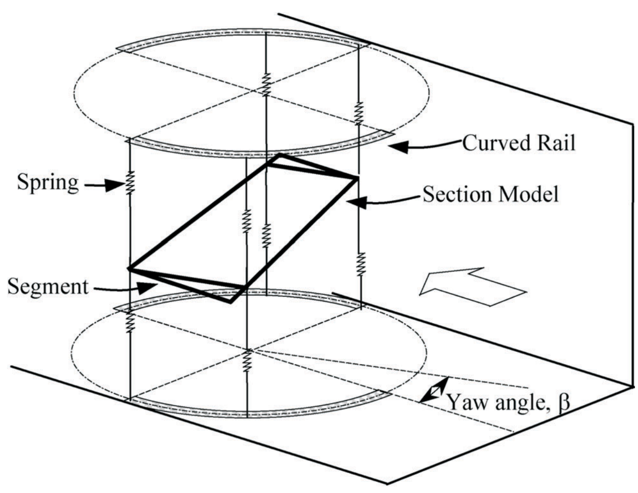

Figure 3. Configuration for measuring flutter derivatives.

for the subsequent bridge flutter and buffeting analysis.

In addition to the measurements of aerodynamic coefficients and flutter derivatives, the flutter critical wind speeds and buffeting responses of the section models with different yaw angles and different angles of wind attack were also measured. The cross sectional properties of the section models are listed in Table 1. The flutter critical wind speeds of the section models were tested in smooth flow and the buffeting responses were tested in a turbulent flow which was generated by a set of grids with the turbulence intensity of 8% and the length scale of 0.1032 m. In the tests for measuring flutter critical wind speeds, the damping ratios of vertical and torsional modes were all 0.4%. Since the frequency ratio between vertical and torsional modes should be maintained as a constant in the tests for measuring buffeting responses. The configuration in these tests was adjusted, the damping ratios of vertical and torsional modes were 1.2% and 1.4%, respectively.

4. Experimental Results

4.1 Aerodynamic Coefficients

For the section model with B/H ratio of 5, the drag, lift, and torsional coefficients C_{Dw}, C_{Lw}, and C_{Mxw} are shown in Figure 4, respectively. It can be seen from Figure 4(a) that the drag coefficients decrease as the yaw angles increase. Due to the symmetrical cross sections, the drag coefficients are nearly symmetrical with respect to angles of wind attack. The results in Figures 4(b) and (c) show that the magnitudes of the lift and torsional coefficients slightly decrease as the yaw angles increase. It should be noted that the lift and torsional coefficients are not anti-symmetric with respect to zero angle of attack. This is due to the inevitable errors in the experiments. However, the discrepancies are minor, the results are still reliable. For the section model with B/H ratio of 10, the drag , lift, and torsional coefficients C_{Dw}, C_{Lw}, and C_{Mxw} are shown in Figure 5, respectively. It can be seen that the trend of these coefficients versus angles of wind attack is similar to that for the section model with B/H ratio of 5.

4.2 Flutter Derivatives

The flutter derivatives, H^*_i and A^*_i (i = 1,4), for the section model with B/H ratio of 5 are shown in Figure 6, respectively. From Figure 6(a),(c),(d), it can be seen that the values of H^*_1, H^*_3, and H^*_4 are all negative and the magnitudes increase with the reduced velocities. The trend of these flutter derivatives with respect to reduced velocities is almost the same for different yaw angles. The magnitudes slightly decrease as the yaw angles increase. From Figure 6(b), it can be inspected that the values of H^*_2 are negative at low reduced velocities and turn into positive values at the reduced velocities of 2.5–4. The values decrease as the yaw angles increase. From Figure 6(e)–(h), it can be seen that the effects of yaw angles on A^*_1, A^*_2, A^*_3, and A^*_4 are not obvious at the low reduced velocities. These effects become more apparent at the higher reduced velocities. However, the discrepancies are not significant. For A^*_1, A^*_3, and A^*_4, a common trend is that the magnitudes decrease as the yaw angles increase. For A^*_2, the values are negative at low reduced velocities and turn into positive values at the reduced velocities of 5–6 where the larger values are for the larger yaw angles. It reveals that for single-degree-of-freedom flutter, the flutter critical wind speeds increase with the yaw angles.

The flutter derivatives, H^*_i and A^*_i (i = 1,4), for the section model with B/H ratio of 10 are shown in Figure 7, respectively. It can be inspected, from this figure, that the relationship between the values and the reduced velocities is similar to that for the section model with B/H ratio of 5. The effects of yaw angles on the flutter derivatives,

Table 1. Cross sectional properties of the section models and the prototype

Properties	Prototype	Model
Width (m)	32	0.26
Mass (kg/m)	39032	2.58
Polar mass moment of inertia (kg-m^2/m)	6762226 (7644813)	0.0295 (0.0334)
Vertical l nature frequency (Hz)	0.328	3.14
Torsional nature frequency (Hz)	0.588	5.63
Torsional-to-vertical frequency ratio	1.79	1.79

* The values in ( ) are used for the case with B/H = 10

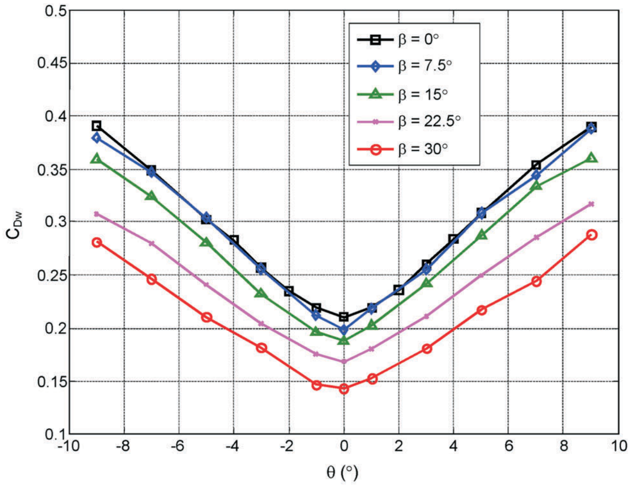

(a) Drag coefficients

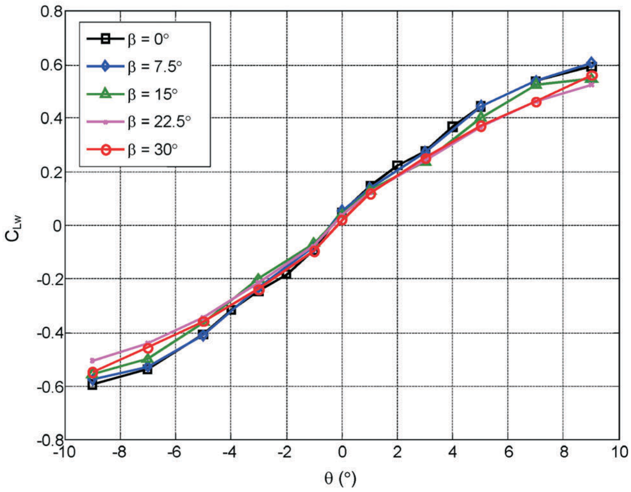

(b) Lift coefficient

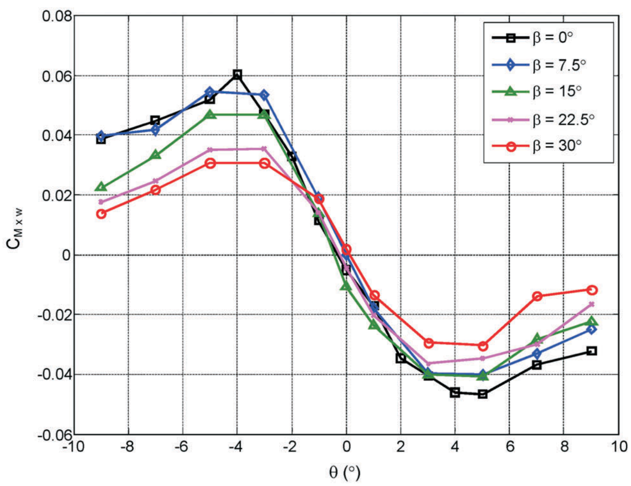

(c) Torsional coefficients

Figure 4. (a) Drag coefficients, (b) Lift coefficient, and (c) Torsional coefficients (B/H = 5).

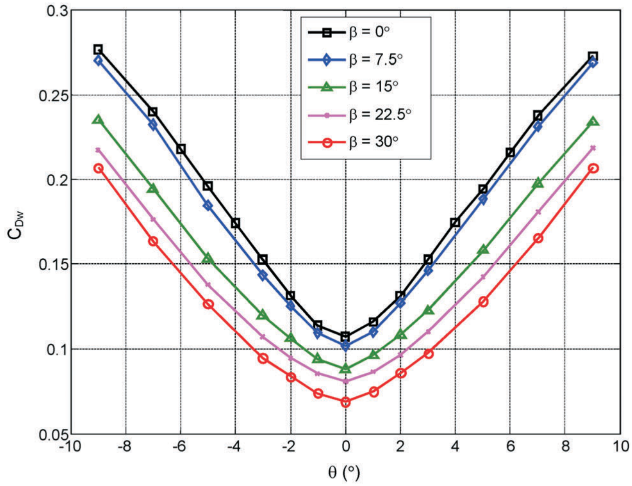

(a) Drag coefficients

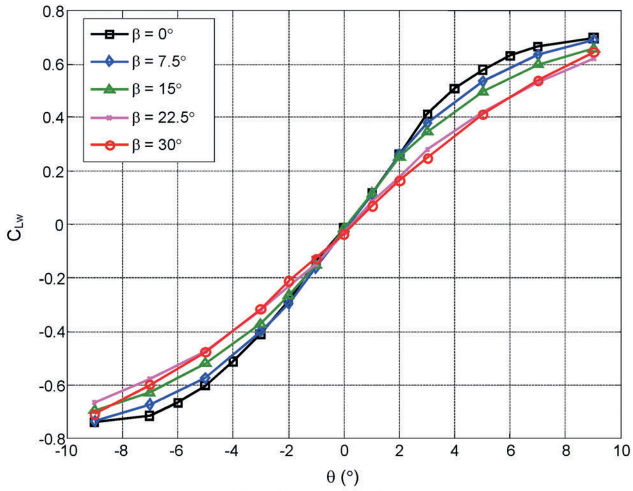

(b) Lift coefficient

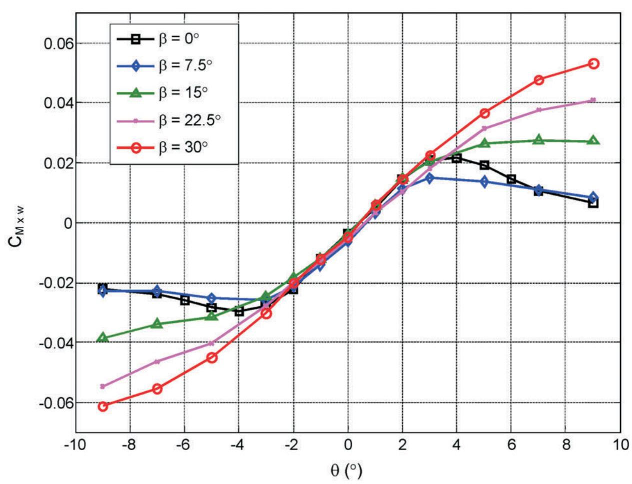

(c) Torsional coefficients

Figure 5. (a) Drag coefficients, (b) Lift coefficient, and (c) Torsional coefficients (B/H = 10).

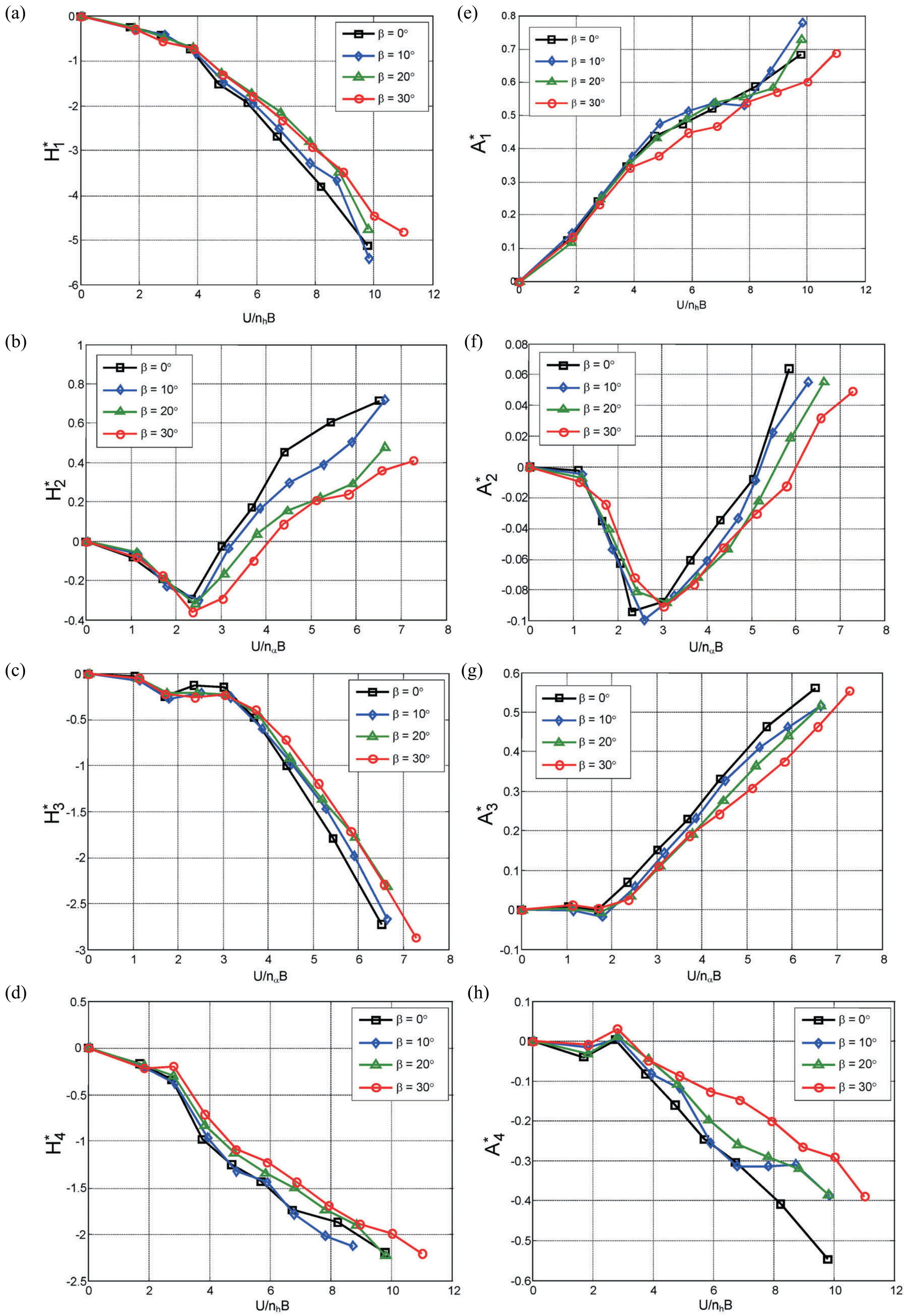

Figure 6. Flutter derivatives (a) H^*_1, (b) H^*_2, (c) H^*_3, (d) H^*_4, (e) A^*_1, (f) A^*_2, (g) A^*_3, and (h) A^*_4 (B/H = 5).

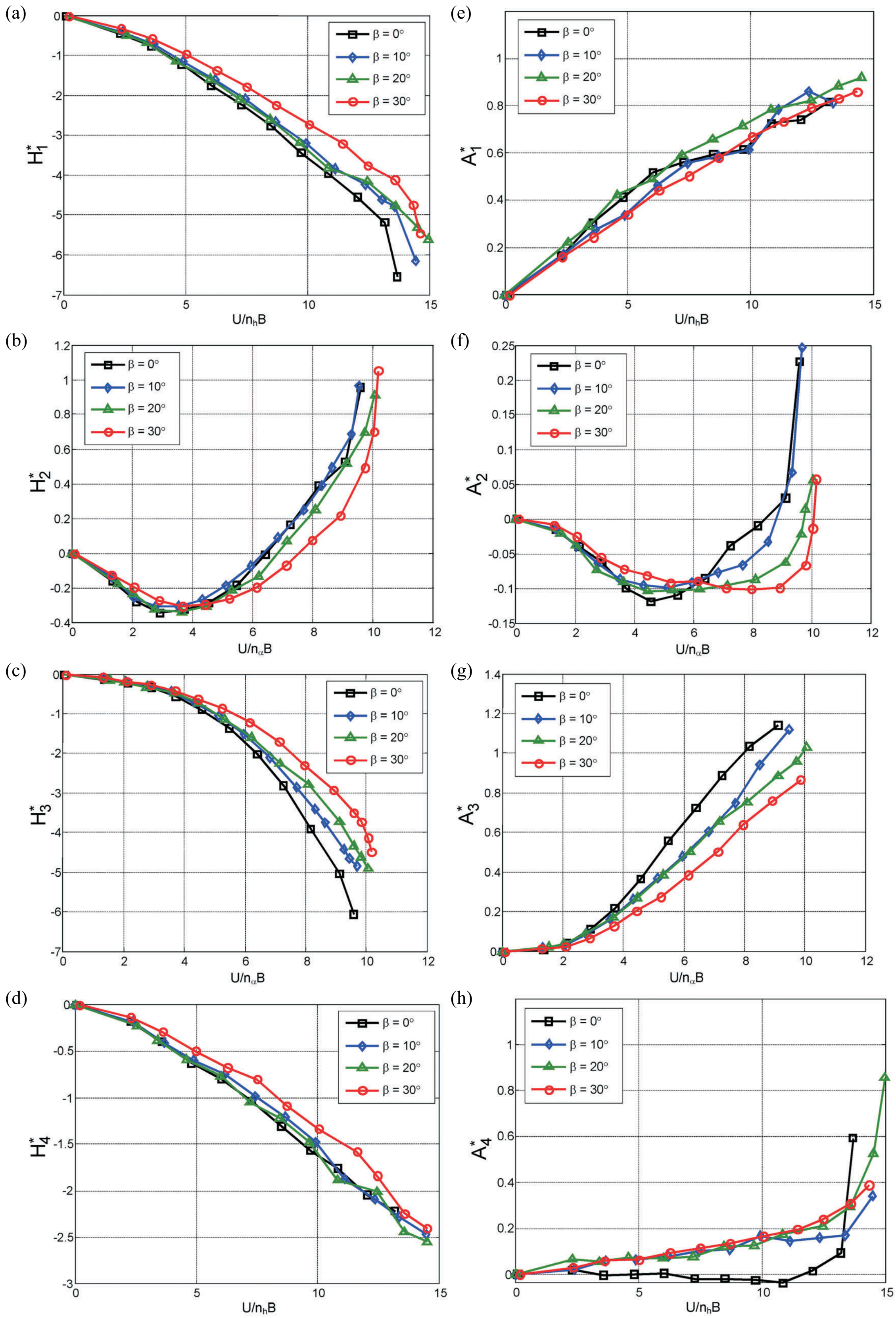

Figure 7. Flutter derivatives (a) H^*_1, (b) H^*_2, (c) H^*_3, (d) H^*_4, (e) A^*_1, (f) A^*_2, (g) A^*_3, and (h) A^*_4 (B/H = 5).

except A^*_4, are also in a similar trend to those in the case with B/H ratio of 5. It can be seen from Figure 7(h) that the values of A^*_4 with zero yaw angle shows different trend from the other cases. In the case of zero yaw angle, the values of A^*_4 are negative and turn into positive at high reduced velocities. In the other cases, the values of A^*_4 are all positive and increase with the reduced velocities.

4.3 Flutter Critical Wind Speeds

When the torsional RMS response reaches to 0.5°, the corresponding wind velocity is regarded as the flutter critical wind speed. The flutter critical wind speeds of the section models for different yaw angles and angles of wind attack are listed in Table 2. For the case with B/H ratio of 5, it can be seen that the lowest flutter critical wind speed occurs at the angle of wind attack of -3 degrees with zero yaw angle. It should be noted that in some cases the flutter critical wind speed does not increase with the yaw angle. For the case with B/H ratio of 10, it can be seen that the flutter critical wind speeds increase with yaw angles for the cases with angles of wind attack of zero degree and 3 degrees only. For the cases with angle of wind attack of -3 degrees, the flutter critical wind speed with the yaw angles of 10 and 20 degrees are lower than that with zero yaw angle. It shows that the lowest flutter critical wind speed occur at the case with the yaw angles of 20 degrees. This phenomenon is similar to that in the reference [2]. The above results also reveal that the effects of yaw angles on the flutter critical wind speeds cannot be estimated by the mean wind decomposition method.

4.4 Buffeting Responses

The section models were tested in a homogeneously turbulent flow with the turbulence intensity of 8%. The test was conducted with the case of zero angle of wind attack. Only the effects of yaw angles were studied. The vertical and torsional responses for the section models with B/H ratios of 5 and 10 are shown in Figure 8–9. Generally speaking, the responses increase with wind speeds. At the same wind speed, the responses reduce as the yaw angles increase. The effects of yaw angles on responses become more obvious as the wind speed increases. From the results, it can be also seen that the flutter wind speed, identified as the sharp increase in torsional response, in turbulent flow is larger than that in smooth flow shown in Table 2. These findings are the same as those in the references [14,15].

5. Numerical Results

5.1 Description of the Bridge

A bridge example is presented to verify the applicability and validity of this approach used in predicting the aerodynamic behavior of the bridge under skew wind. The properties of the section models in the wind tunnel test were determined by following the similitude rule with the prototype bridge used here. The properties of the bridge deck are depicted in Table 1. The bridge has two spans with the span lengths of 150 and 275 m, respectively (shown in Figure 10). Two types of bridge decks of rectangular cross sections with B/H ratios of 5 and 10 are used. The cables, anchored at tower and bridge deck, are arranged in the middle plane of the bridge. A finite element analysis was employed to analyze the structural modes and their natural frequencies. There are 41 beam elements, used to model the bridge deck and the tower, and 20 cable elements, used to model the cables, in the analysis. Although the mass moments of inertia used in these two types of deck cross sections are slightly different, the corresponding torsional constants are adjusted to make the natural frequencies of the bridges with these two types of deck cross sections to be

Table 2. Flutter critical wind speeds of the section models

Angle of Wind	B/H = 5				B/H = 10			
	Yaw Angles (°)				Yaw Angles (°)			
Attack (°)	0	10	20	30	0	10	20	30
-3	4.6	4.7	4.8	5.4	6.0	5.6	5.5	6.1
0	4.9	4.9	4.9	5.4	7.8	8.0	8.3	8.6
3	4.9	4.9	4.9	5.6	5.9	6.0	5.9	6.8

* U/n_tB, n_t is the natural frequency of torsional mode.

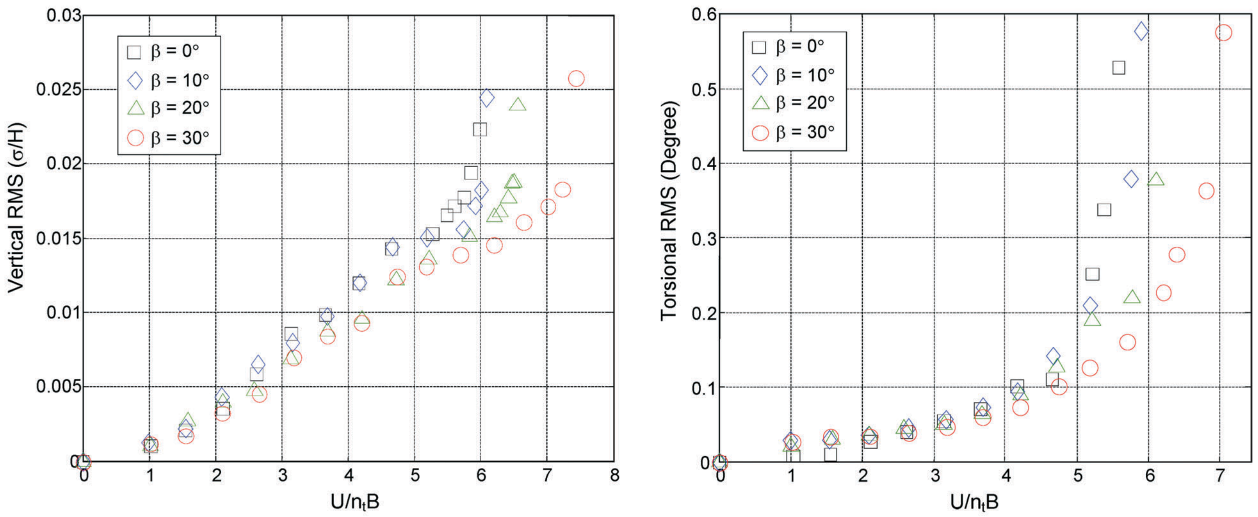

(a) vertical responses (b) torsional responses

Figure 8. Measured buffeting responses for different yaw angles (a) vertical responses and (b) torsional responses (B/H = 5).

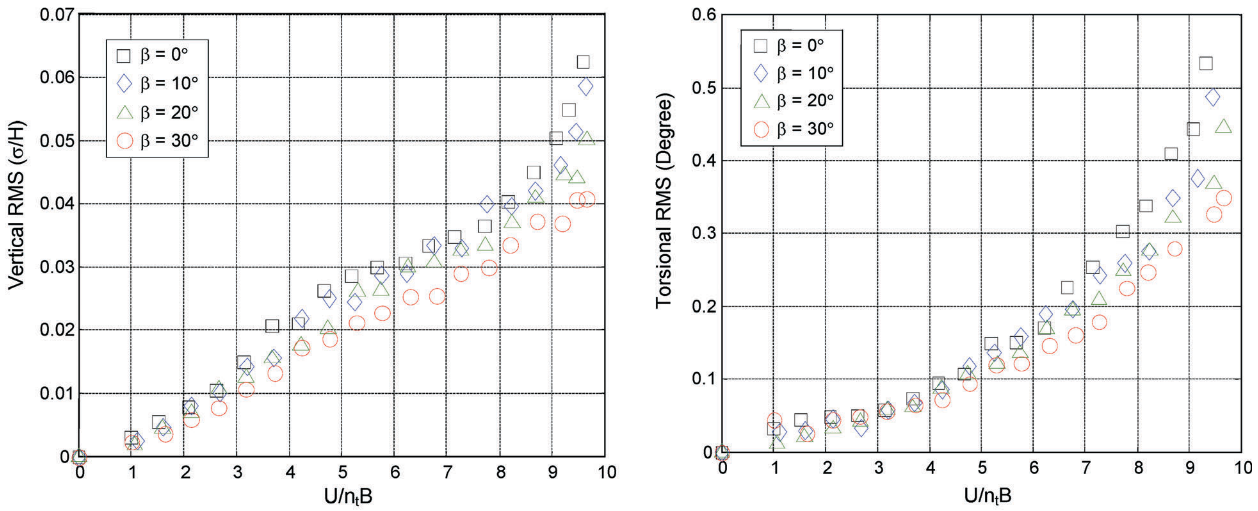

(a) vertical responses (b) torsional responses

Figure 9. Measured buffeting responses for different yaw angles (a) vertical responses and (b) torsional responses (B/H = 10).

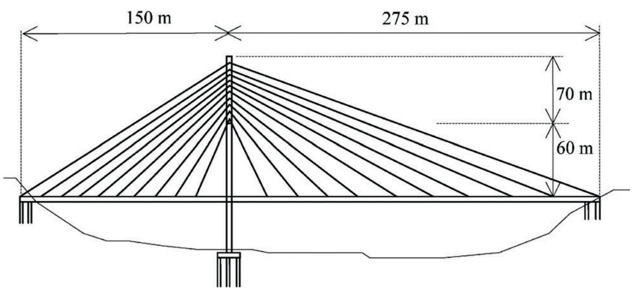

Figure 10. Geometry of the bridge used in example.

the same. The results of first ten modes are listed in Table 3. The natural frequency ratio between the first torsional mode and the first vertical mode is 1.8 that is used in the section model test. In this analysis, the aerodynamic coefficients and flutter derivatives obtained from the section model test are adopted. For the buffeting analysis, the wind speed spectra in the longitudinal and vertical directions are expressed as follows [11]:

$$\frac{nS_u(z,n)}{u_*^2} = \frac{200f}{(1+50f)^{5/3}} \tag{12}$$

$$\frac{nS_w(z,n)}{u_*^2} = \frac{3.36f}{1+10f^{5/3}} \tag{13}$$

The lateral turbulence was neglected in this analysis.

Table 3. Natural frequencies of first ten modes of the example

Mode	Frequency (Hz)	Dominant axis	Mode	Frequency (Hz)	Dominant axis
1	0.328	Lift (S)	6	0.953	Lift (AS)
2	0.588	Torsional (S)	7	1.078	Torsional (AS)
3	0.614	Tower	8	1.166	Torsional (AS)
4	0.707	Lift (AS)	9	1.172	Lift (AS)
5	0.790	Drag (S)	10	1.437	Lift (S)

* S – Symmetric, AS – Anti-symmetric.

5.2 Flutter Critical Wind Speeds

The calculated flutter wind speeds of the bridge under different yaw angles are shown in Table 4. From this table, it shows that the flutter critical winds increase with the yaw angles for both deck cross sections. The trend is similar to that in the test shown in Table 2. The effects of yaw angles in the numerical analysis seem to be more significant than those in the test. One of the reasons is due to the flutter derivative A^*_2. Figure 6(f) shows that the wind speeds corresponding to the sign change of A^*_2 for different yaw angles are more distinct than those in the test. The other reason is the difference of mode shapes. The distribution of mode shapes along bridge axis cannot be included in the section model test.

5.3 Buffeting Responses

The calculated buffeting responses of the bridge under skew wind in the drag, lift, and torsional directions are plotted in Figure 11–12, respectively. From these figures, the responses increase with wind speeds and at the same wind speed the responses reduce as the yaw angles increase. The trend is conforming to that in the test shown in Figure 8–9. For comparison, the responses obtained from the mean wind decomposition method are also shown in these figures. For the case with B/H ratio of 5, the vertical responses obtained from decomposition method agree well with those obtained from this approach. However, the decomposition method underestimates the torsional responses. The maximum differences are approximately 20%. This reveals that the decomposition method is not applicable to the case with B/H ratio of 5. For the case with B/H ratio of 10, the vertical and torsional responses obtained from decomposition method agree well with those obtained from this approach.

6. Conclusion

The aerodynamic behavior of bridges under skew winds was studied in this paper. Two types of deck cross sections, with B/H ratios of 5 and 10, were used in the test and the numerical analysis. From the results obtained from the test and the numerical analysis, some conclusions can be drawn as follows:

(1) The experimental results show that for the section model with B/H ratio of 5, the lowest flutter wind speed occurs at a negative angle of wind attack and a zero yaw angle. For the section model with B/H ratio of 10, the lowest flutter wind speed occurs at a negative angle of wind attack and a yaw angle of 20 degrees. In the cases of zero angle of wind attack for both section models, the flutter critical wind speeds increase with the yaw angles.

(2) For both the section models, the results obtained from the tests indicate that the buffeting responses decrease as the yaw angles increase.

(3) The effects of yaw angles on the calculated and experimental results follow the same trend both in the flutter critical wind speeds and the buffeting responses. It reveals that the analytical approach based on the flutter derivatives and aerodynamic coeffi-

Table 4. Flutter critical wind speeds of the prototype (m/s)

Angle of Wind	B/H = 5				B/H = 10			
	Yaw Angles (°)				Yaw Angles (°)			
Attack (°)	0	10	20	30	0	10	20	30
0	94.5	103.2	106.2	113.7	128.8	146.3	156.1	171.1

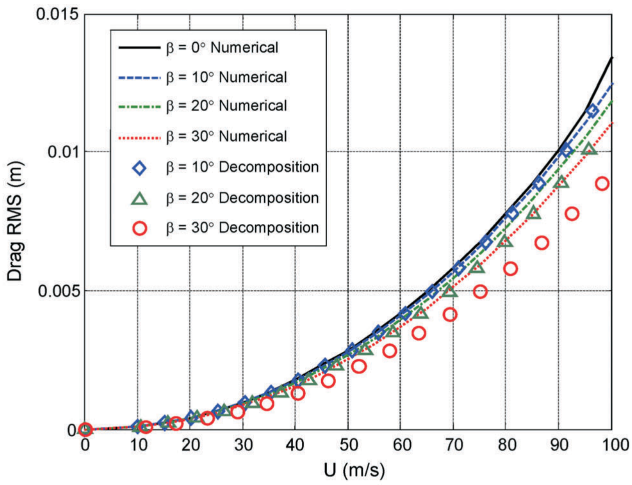

(a) drag responses

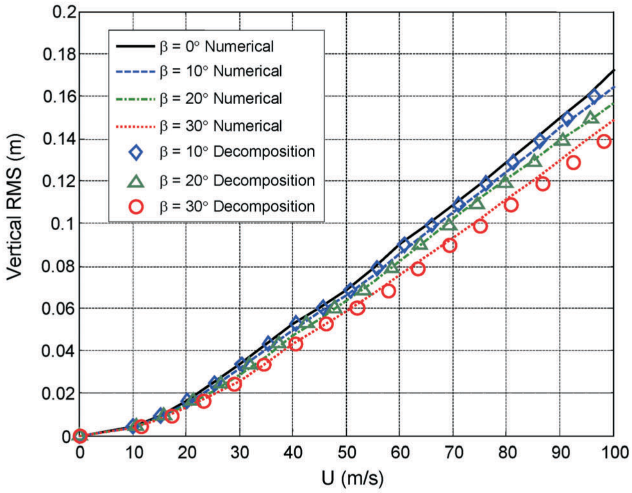

(b) vertical responses

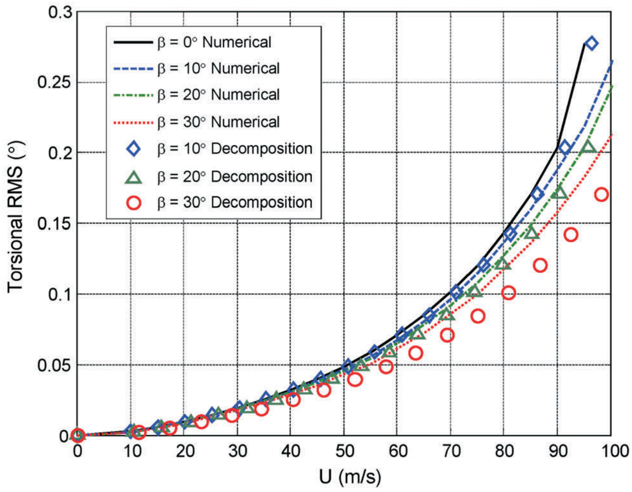

(c) torsional responses

Figure 11. Calculated buffeting responses for different yaw angles (a) drag responses, (b) vertical responses, and (c) torsional responses (B/H = 5).

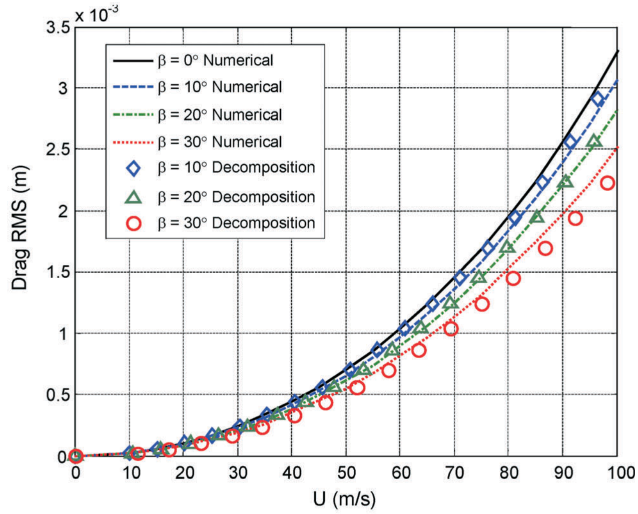

(a) drag responses

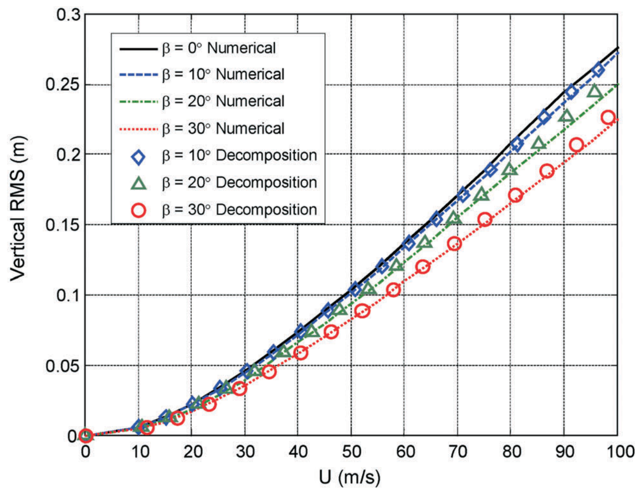

(b) vertical responses

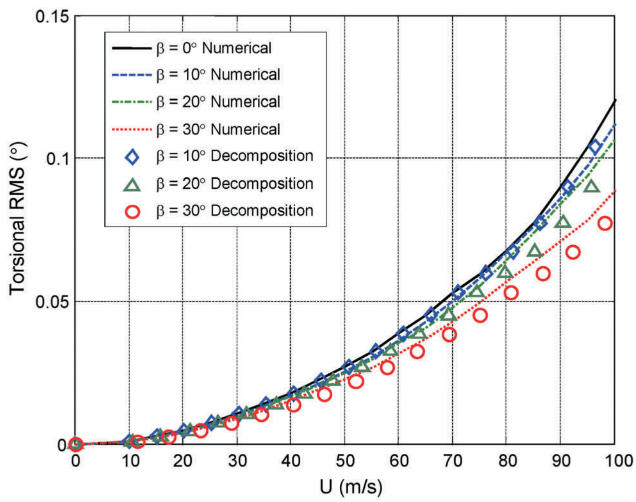

(c) torsional responses

Figure 12. Calculated buffeting responses for different yaw angles (a) drag responses, (b) vertical responses, and (c) torsional responses (B/H = 10).

cients obtained from the section models under skew wind is valid and applicable.

(4) The conventional mean wind decomposition method underestimates the torsional buffeting responses in the case of B/H ratio of 5. However, the conventional method is applicable to the case of B/H ratio of 10 for predicting buffeting responses.

References

[1] Tanaka, H. and Davenport, A. G., "Results of Taut Strip Models to Turbulent Wind," *Journal of Engineering Mechanics-ASCE*, Vol. 108, pp. 33–49 (1982).

[2] Zhu, L. D., Wang, M., Wang, D. L., Guo, Z. S. and Cao, F. C., "Flutter and Buffeting Performances of Third Nanjing Bridge over Yangtze River under Yaw Wind via Aeroelastic Model Test," *Journal of Wind Engineering and Industrial Aerodynamics*, Vol. 95, pp. 1579–1606 (2007).

[3] Zhu, L. D. and Chang, G. Z., "Study of Flutter Performance of Flat Box Deck Bridge under Skew Wind via Wind Tunnel Test," *Journal of Bridge Construction*, Vol. 2, pp. 7–10 (2006) (in Chinese).

[4] Xie, J. and Tanaka, H., "Buffeting Analysis of Long Span Bridges to Turbulent Wind with Yaw Angle," *Journal of Wind Engineering and Industrial Aerodynamics*, Vol. 37, pp. 65–77 (1991).

[5] Kimura, K. and Tanaka, H., "Bridge Buffeting Due to Wind with Yaw Angles," *Journal of Wind Engineering and Industrial Aerodynamics*, Vol. 42, pp. 1309–1320 (1992).

[6] Zhu, L. D., Xu, Y. L., Zhang, F. and Xiang, H. F., "Tsing Ma Bridge Deck under Skew Winds — Part I: Aerodynamic Coefficients," *Journal of Wind Engineering and Industrial Aerodynamics*, Vol. 90, pp. 781–805 (2002).

[7] Zhu, L. D., Xu, Y. L. and Xiang, H. F., "Tsing Ma Bridge Deck under Skew Winds — Part II: Flutter Derivatives," *Journal of Wind Engineering and Industrial Aerodynamics*, Vol. 90, pp. 807–837 (2002).

[8] Xu, Y. L. and Zhu, L. D., "Buffeting Response of Long-Span Cable-Supported Bridges under Skew Winds. Part 2: Case Study," *Journal of Sound and Vibration*, Vol. 281, pp. 647–673 (2005).

[9] Ding, Q. Y., Zhou, Z. Y., Zhu, L. D. and Xiang, H. F., "Identification of Flutter Derivatives of Bridge Decks with Free Vibration Technique," *Journal of Wind Engineering and Industrial Aerodynamics*, Vol. 98, pp. 12–23 (2010).

[10] Scanlan, R. H., "Estimates of Skew Wind Speeds for Bridge Flutter," *Journal of Bridge Engineering*, Vol. 4, pp. 95–98 (1999).

[11] Simiu, E. and Scanlan, R. H., *Wind Effects on Structures*, 2nd ed., John Wiley & Sons, New York (1996).

[12] Sarkar, P. P., Jones, N. P. and Scanlan, R. H., "System Identification for Estimation of Flutter Derivatives," *Journal of Wind Engineering and Industrial Aerodynamics*, Vol. 42, pp. 1243–1254 (1992).

[13] Piccardo, G., Carassale, L. and Freda, A., "Critical Conditions of Galloping for Inclined Square Cylinders," *Journal of Wind Engineering and Industrial Aerodynamics*, Vol. 99, pp. 748–756 (2011).

[14] Lin, Y. Y., Cheng, C. M. and Lan, C. Y., "Effects of Deck's Width-to-Depth Ratios and Turbulent Flows on the Aerodynamic Behaviors of Long-Span Bridges," *Wind and Structures*, Vol. 6, pp. 263–278 (2003).

[15] Lin, Y. Y., Cheng, C. M., Wu, J. C., Lan, T. L. and Wu, K. T., "Effects of Deck Shape and Oncoming Turbulence on Bridge Aerodynamics," *Tamkang Journal of Science and Engineering*, Vol. 8, pp. 43–56 (2005).

Manuscript Received: Jan. 12, 2012
Accepted: Apr. 6, 2012